Journal of Materials Chemistry C

Accepted Manuscript

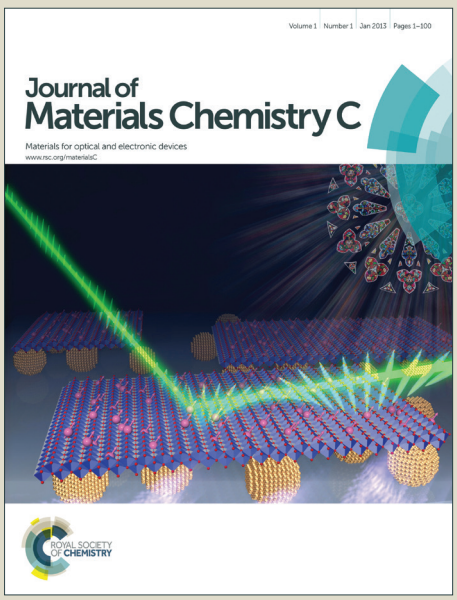

ROYAL SOCIETY OF CHEMISTRY

www.rsc.org/materialsC

Cite this: DOI: 10.1039/c0xx00000x

www.rsc.org/xxxxxx

ARTICLE TYPE

Pentacenequinone Derivatives: Aggregation-Induced Emission Enhancement, Mechanism and Fluorescent Aggregates for Superamplified Detection of Nitroaromatic Explosives

Sandeep Kaur,[§] Ankush Gupta,[§] Vandana Bhalla* and Manoj Kumar

Received (in XXX, XXX) Xth XXXXXXXXX 20XX, Accepted Xth XXXXXXXXX 20XX
DOI: 10.1039/b000000x

Pentacenequinone derivatives **5-9** have been synthesized by Suzuki-Miyaura coupling protocol. These derivatives form fluorescent aggregates in mixed aqueous media due to their aggregation-induced emission enhancement (AIEE) attributes. Interestingly, size dependent emission enhancement is observed in case of derivatives **5-7** and the effect of increase in number of pyridine rotors on fluorescence emission of pentacenequinone derivatives **6-7** in solution and in aggregate state confirms that AIEE phenomenon is at the cost of aggregation driven growth and restriction of intramolecular rotation (RIR). On the other hand, derivatives **8** and **9** having electron rich phenyl groups are donor-accepter-donor type systems which exhibit intermolecular charge transfer state (ICT) and form fluorescent aggregates in mixed aqueous media. In addition to this, the AIEE characteristics endow pentacenequinone derivatives **5-9** with sensing functionality such as detection of nitroaromatic compounds. TLC strips of AIEE-active pentacenequinone derivatives **5-9** provide a more convenient and cost-effective approach for the trace detection of nitroaromatic explosives.

Introduction

Highly luminescent π-conjugated organic molecules form the basis of optical and electronic devices such as organic light-emitting diodes (OLEDs),[1] organic light-emitting field-effect transistors (OLEFETs)[2] and organic fluorescent sensors.[3] However, most π-conjugated molecules have very high efficiency in dilute solution but relatively weak emission in solid state as intra- and intermolecular interactions quench the emission process.[4] Several approaches such as dendritic or bulky substituent protection,[5, 6] cross dipole stacking,[7] aggregation-induced emission,[8] *J*-aggregate formation[9] and enhanced intramolecular charge-transfer transition[10] have been used to achieve an intense solid-state emission. A variety of organic molecules such as siloles,[11, 12] 1-cyano-*trans*-1,2-bis(4-methylbiphenyl)ethylene,[13] thienyl-azulene,[14] arylethene[15] and naphthalimide[16] derivatives that emit strongly in their aggregated or solid state have been reported. Various possible mechanisms including conformational planarization, *J*-aggregate formation, twisted intramolecular charge transfer (TICT) and restriction of intramolecular rotation (RIR) have been proposed for the increase in emission intensity in aggregated state.[17-21] Thus, more investigation is needed to prove the actual mechanism for the aggregation-induced emission enhancement (AIEE) phenomenon.

Our research work involves design, synthesis and evaluation of organic materials having AIEE characteristics for the detection of various analytes.[22-25] In our previous reports, we have utilized the AIEE phenomena for the preparation of fluorescent aggregates. Further we utilized these aggregates for detection of nitroaromatic explosives viz. picric acid (PA) and trinitrotoluene (TNT). However, in none of these reports we have discussed the effect of nature and number of rotors on the photophysical properties of these derivatives in aggregated state. In addition, we have not discussed the reason of AIEE phenomena in these molecules. Since most of these reported derivatives form spherical aggregates, we could not study the relationship between morphology of these derivatives with their sensing sensitivity toward nitroaromatic explosives. In one of the published research work, we reported that pentacenequinone derivative **6** forms fluorescent aggregates in aqueous media due to its AIEE attributes.[23] We proposed that RIR[26] of the hetero-aromatic ring at the periphery of pentacenequinone core in aggregated state is the main cause of AIEE effect. To get more insight into the mechanism of AIEE, in the present manuscript, we have designed and synthesized a series of new AIEE-active molecules based on pentacenequinone scaffold. We have chosen pentacenequinone scaffold as it is rigid and planar molecule and has tendency to form ordered thin films which make it good candidate for preparation of organic electronic devices.[27] We envisioned that varying the number of hetero-aromatic rotors on pentacenequinone core would influence photophysical properties of the molecules which will be helpful in understanding the mechanism of AIEE and hence will provide the molecular designs for the preparation of fluorescent aggregates.[28,29] Thus, with this hypothesis in mind, we designed and synthesized *mono*, *di* and *tetra* substituted pentacenequinone derivatives **5-7**. We observed that in

aggregated state emission intensity of these derivatives increased with increase in number of pyridine rotors on pentacenequinone core. Further, comparison of fluorescence studies of derivatives **6-7** suggest that AIEE phenomenon is due to aggregation driven-growth and restriction of intramolecular rotation. In addition to this, we synthesized the pentacenequinone based derivatives **8** and **9** and found that these derivatives are donor-accepter-donor type systems which exhibit intermolecular charge transfer state (ICT) and form fluorescent aggregates in mixed aqueous media. Presence of alkyl chains on pentacenequinone derivative **8** enhances the emission efficiency in aggregated state as compared to derivative **9**. Further, we utilized TLC strips coated with derivatives **5-9** for instant detection of nitroaromatic explosives.

Results and Discussion

Pentacenequinone derivatives **5-7** were synthesized by Suzuki-Miyaura coupling of boronic ester **4a**[30] with respective pentacenequinone derivatives **1-3**[31, 32] (Scheme 1). The structures of derivatives **5, 6**[23] and **7** were confirmed from their spectroscopy and analytical data (Fig. S44-S47 in ESI†).

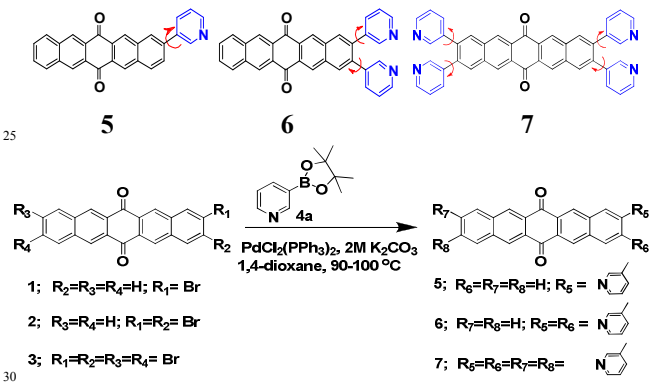

Scheme 1. Pentacenequinone based derivatives **5-7**.

We evaluated the photophysical properties of pentacenequinone derivatives **5-7** by UV-vis and fluorescence spectroscopy. The UV-vis spectrum of derivative **5** in DMSO exhibits characteristic absorption band at 310 nm corresponding to π-π* transition of pentacenequinone moiety (Fig. S1 in ESI†). On addition of water fractions (up to 50%) to the DMSO solution of derivative **5**, *level-off* long wavelength tail appears which is attributed to the Mie scattering due to formation of aggregates[33] (Fig. S1 in ESI†). Similar results were obtained in case of pentacenequinone derivatives **6** and **7** under same set of conditions as used for derivative **5** (Fig. S2-S3 in ESI†).

In the fluorescence spectrum, the dilute solution of derivative **5** in DMSO exhibits weak emission band (Φ_F[34] = 0.030) at 460 nm when excited at 310 nm (Fig. 1). However, a dramatic change in fluorescence emission intensity is observed in H_2O/DMSO mixture. On addition of 10% volume fraction of water an emission band appears at 468 nm. Addition of 30% volume fraction of water leads to enhancement of emission along with red shift in the emission band from 468 nm to 481 nm (Δλ=13 nm). Further addition of water fractions up to 50% leads to enhancement in emission intensity which is clearly visible to naked eye under the illumination of 365 nm (inset, Fig. 1). The scanning electron microscopy (SEM) analysis of derivative **5** in H_2O /DMSO (1:1, v/v) mixture showed the presence of irregular shaped aggregates (Fig. S4A in ESI†). The dynamic light scattering (DLS) studies clearly showed average size around 660 nm, 440 nm and 220 nm in 10%, 30%, and 50% H_2O/DMSO solvent mixture of derivative **5** respectively (Fig. S4B in ESI†). We assume that as the particles tend to shrink in size with increasing water content in the solvent mixture,[35] a more coplanar conformer imposed by the congested environment in the shrunk particles may be responsible for this bathochromic shift.

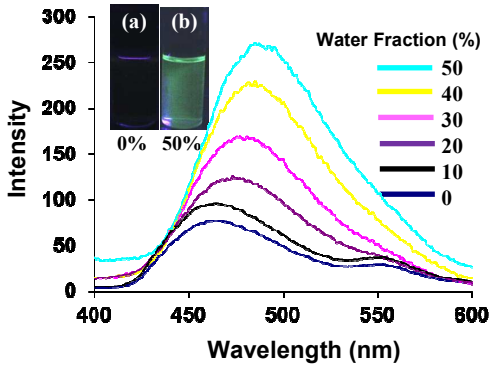

Fig. 1 Fluorescence spectra of derivative **5** (10 μM) showing the variation of fluorescence intensity in H_2O/DMSO mixtures. λex. =310 nm. Inset photograph shows the fluorescence intensity at (a) 0% (b) 50% water in DMSO.

However, addition of more than 50% water fraction to DMSO solution of derivative **5** results in decrease in fluorescence emission intensity (Fig. S5 in ESI†). This phenomenon is often observed in derivatives with AIEE properties[36] as after the aggregation only the molecules on the surface of aggregate emit light and contribute to the fluorescent intensity upon excitation and this leads to a decrease in emission intensity.[36] We also carried out fluorescence studies of pentacenequinone derivatives **6**[23] and **7** under same set of conditions as used for derivative **5** (Fig. S5 and S6 in ESI†). Addition of water fractions up to 50% to the DMSO solution of derivative **7** leads to red shifting (Δλ=28 nm) of emission band from 464 to 492 nm along with enhancement of the emission signal. The DLS studies of derivative **7** in 10%, 30%, and 50% H_2O/DMSO solvent mixture showed aggregates of average size around 305 nm, 550 nm and 768 nm, respectively (Fig. S7A in ESI†). The enhancement and red shifting of the emission signal is related to the aggregation driven growth of the aggregates[14] of derivative **7**. A linear relationship between emission enhancement and size of aggregates of derivative **7** is observed (Fig. S8A in ESI†). Similar emission behaviour is observed in case of derivative **6** (Fig. S7B and S8B in ESI†). The SEM image of derivative **6** showed irregular shaped aggregates whereas flake like morphology was observed in case of derivative **7** (Fig. S9A and S9B in ESI†).

The quantum yield of aggregates of derivative **7** in H_2O/DMSO (1:1, v/v) increased to 0.43 which is 16 times higher than that in DMSO solution. In case of derivative **6** and **5**, an increase of 14 and 7 times respectively is observed to that of their DMSO solutions.

To get insight into the mechanism of AIEE, we investigated the

Derivative	λ_{max} [a]	Quantum yield (Φ_F)[b] in solution	Quantum yield (Φ_F)[c] in aggregates	Emission enhancement	I/I_0 [d]	$(I-I_0)/I_0$ x100 [e]	A_1/A_2 [f]	τ_{F1} [g] (ns)	τ_{F2} [g] (ns)	K_f [h] ($10^9 s^{-1}$)	K_{nr} [i] ($10^9 s^{-1}$)
5	481	0.030	0.22	7.3(Φ_F^c/Φ_F^b)	5.6	48	72/28	0.30	2.02	0.733	2.6
6	481	0.029	0.41	14.13(Φ_F^c/Φ_F^b)	9.56	74	36/64	0.078	1.63	0.251	0.36
7	492	0.027	0.43	15.92(Φ_F^c/Φ_F^b)	11.8	82	35/65	0.13	1.84	0.233	0.30

Table 1 Comparative photophysical properties of derivative **5-7**: [a] emission maximum (nm). [b] solution in DMSO [c] aggregates in H_2O/DMSO with 50 vol% of water. [d] increase in fluorescence intensity in 90% volume fraction of glycerol in DMSO. [e] decrease in % age fluorescence intensity with increase in temperature upto 75^{0}C in 50 vol% of water in DMSO. [f] A_1, A_2 : fractional amount of molecules in each environment. [g] $\tau_{F1 \text{ and }} \tau_{F2}$: biexponential life time of aggregates in 50 vol% of water in DMSO. [h] radiative rate constant ($K_f = \Phi_F/\tau_F$). [37] [i] non-radiative rate constant ($K_{nr} = (1-\Phi_F)/\tau_F$).[37]

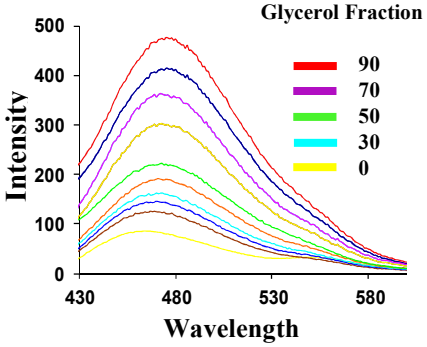

Fig. 2 Fluorescence spectra of derivative **5** (5 μM) showing the variation of fluorescence intensity in DMSO/glycerol mixtures with different glycerol fractions.

effect of variations in the viscosity and temperature on fluorescence behaviour of derivatives **5-7**. For this, the fluorescence spectra of derivative **5** in viscous mixture of DMSO and glycerol with different glycerol fractions were recorded (Fig. 2) and it was found that upon addition of 90% volume fraction of glycerol, the fluorescence intensity increases. This is attributed to high viscosity that hampers intramolecular rotation, leading to closure of the non-radiative decay channel, hence, making the molecule emissive. In 50% DMSO/glycerol solvent mixture, increase in fluorescence emission is purely due to viscosity effect as the derivative is soluble in this mixture. Abrupt increase in fluorescence intensity is observed in presence of more than 50% volume fraction of glycerol in DMSO. This is due to the combined effect of viscosity and aggregation as molecules are less soluble in these mixtures. Similar results were obtained in case of pentacenequinone derivatives **6** and **7** (Fig. S10 in ESI†).

To compare the increase in fluorescence intensity of these derivatives, we plotted the change in peak intensity vs. glycerol content (Fig. S11 in ESI†). Interestingly, fluorescence intensity of derivative **7** increased by 11.8 times to that in pure DMSO solution (Table 1) compared to the 9.56 fold enhancement observed in case of derivative **6**, 5.6 fold enhancement is observed in case of **5**. This may be attributed to greater degree of the restriction in rotation of higher number of rotors.

We investigated the effect of temperature on the fluorescence spectra of derivative **5** in H_2O/DMSO (1:1, v/v) solvent mixture and found that fluorescence intensity decreases with increase in the temperature up to 75°C which clearly shows conversion of aggregated state to a monomer like state at high temperature (Fig. S12 in ESI†). At high temperature pyridine rotors of pentacenequinone derivatives **5-7** rotate fast which lead to non-radiative decay process and hence make them less emissive. Similar results were obtained in case of derivatives **6** and **7** (Fig. S13 in ESI†). The decrease in fluorescence intensity of derivative **7** with increase in solution temperature was up to 82%. On the other hand, decrease of 74% and 48% is observed in case of derivatives **6** and **5** respectively (Table 1). The viscosity and temperature dependent studies suggest that RIR plays a crucial role in emission enhancement in case of derivatives **5-7**.

We carried out time resolved fluorescence studies to determine the life times of these derivatives in the aggregated state. The fluorescence life time data (Table 1) for derivatives **5-7** in the aggregated state were obtained by fitting the time resolved curves based on double-exponential function. Although there is small difference between fluorescence radiative rate constants [37] (K_f) of derivative **5** (0.733×10^9 s^{-1}), **6** (0.251×10^9 s^{-1}) and **7** (0.233×10^9 s^{-1}), the non-radiative decay constant (K_{nr}) of derivative **5** (2.6×10^9 s^{-1}) was larger than those of derivatives **6** (0.36×10^9 s^{-1}) and **7** (0.30×10^9 s^{-1}). These studies show that increase in number of rotors accelerate the decrease in non-emissive rate constant.[37, 38] In case of derivatives **6** and **7**, in aggregated state major fraction of molecules undergo radiative decay through the slow pathway. On the other hand, in case of derivative **5**, 72% of molecules undergo radiative decay through the fast pathway. However, the decay time of derivative **5** in 50% water fraction (0.30 ns) is longer than that of **5** in 0% water fraction (0.081 ns) which implies formation of ordered aggregates.[39] We also carried out the fluorescence anisotropy studies[40-42] of derivative **7** which show an increase in average anisotropy value of derivative **7** in DMSO from 0.05 to 0.32 in H_2O/DMSO (1:1, v/v) (Fig. S14 and S15 in ESI†). This result suggest decreased molecular motion in case of derivative **7** on aggregation.

In the next part of our investigation, we were interested in studying the effect of presence of electron rich phenyl rotors instead of electron deficient rotors on the AIEE characteristics of pentacenequinone derivatives. In view of this, we synthesized pentacenequinone derivatives **8** and **9** with or without alkyl chain respectively by Suzuki-Miyaura coupling of boronic esters **4b**[43] and **4c**[44] with pentacenequinone derivative **2** (Scheme 2). The structures of these derivatives were confirmed from their spectroscopy and analytical data (Fig. S48-S53 in ESI†).

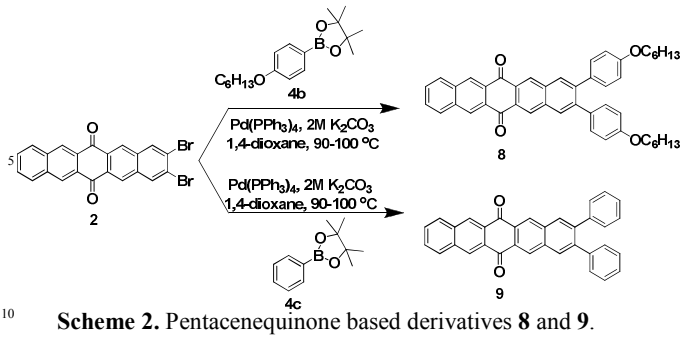

Scheme 2. Pentacenequinone based derivatives **8** and **9**.

We evaluated the aggregation behaviour of derivatives **8** and **9** by UV-vis and fluorescence spectroscopy. Absorption spectrum of dilute solution of derivative **8** in THF shows characteristic absorption band at 300 nm corresponding to π-π* transition of pentacenequinone moiety (Fig. S16A in ESI†). However, in presence of water as co-solvent, a new absorption band at 420 nm is observed along with appearance of level-off long wavelength tail (Fig. S16A in ESI†). This new band may be assigned to intermolecular charge-transfer (ICT) state.[4,45] Similar results were obtained in case of derivative **9** under same set of conditions as used for derivative **8** (Fig. S16B in ESI†). We carried out SEM analysis of derivative **8** and **9** which shows spherical aggregates in H_2O/THF mixture (Fig. S17A and S17B in ESI†).

Further, solution of derivative **8** in THF is weakly emissive when excited at 300 nm (Φ_F = 0.0039). A dramatic change in fluorescence behaviour of derivative **8** is observed when water is added to the THF solution of derivative **8** (Fig. 3). The addition of 60% volume fraction of water to the THF solution of derivative **8** shows dual emission along with enhancement of emission intensity (Fig. 3). The two emission maxima at 475 and 555 nm resulted from locally excited state and intermolecular charge-transfer state, [45] respectively. However, abrupt increase in fluorescence intensity of the emission band at 555 nm is observed (Φ_F = 0.24) on increasing the water content to 90%. This change is clearly visible to naked eye under the illumination of 365 nm light (inset, Fig. 3). We believe that formation of ICT state and conformational fixation upon aggregate formation is the reason for emission enhancement.[46]

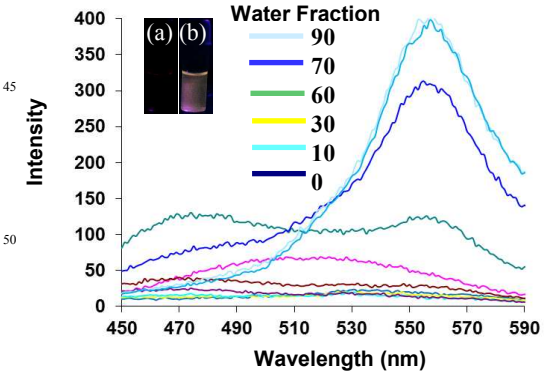

Fig. 3 Fluorescence spectra of **8** (10 μM) showing the variation of fluorescence intensity in H_2O/THF mixtures with different water fractions. Inset photographs (Under 365 nm UV-light) (a) in pure THF (b) with the addition of 90% water in THF.

Similar results were obtained in case of derivative **9** under same set of conditions as used for derivative **8** (Fig. S18 in ESI†). We carried out the fluorescence life time studies of derivatives **8** and **9** to get insight into the nature of excited state (Table S1 pS14 in ESI†), The time resolved fluorescence studies showed increase in life time of derivative **8** from 0.95 ns in THF solution to 3.53 ns in aggregated state and a large increase in fluorescence rate constant from 4.07 x 10^6 s^{-1} in solution to 6.7 x 10^7 s^{-1} in aggregated state (Table S2 pS14 in ESI†). Further, we monitored the fluorescence decay of derivative **8** in H_2O/THF (7/3) at two different emission maxima[45] (Table S1 pS14 in ESI†). The τ_F values (2.82 and 3.07 ns) observed at 555 nm were correspondingly longer than those observed (0.28 and 1.96 ns) at 480 nm. Further, the decay times of 3.07 and 6.54 ns were measured when the H_2O/THF ratios were 7/3 and 9/1, respectively. We believe that longer τ_F values originates from the ICT state as charge transfer state of organic molecules generally exhibits a longer decay time as compared to locally excited state. Interestingly, aggregates of derivative **9** showed higher life time (9.48 ns) than that of aggregates of derivative **8**. This may be attributed to effective π-stacking of phenyl groups in case of derivative **9** as the presence of alkyl side chains in derivative **8** prevent the interchain π-stacking.[47] These studies show that derivatives **8** and **9** are donor-acceptor-donor type systems exhibit ICT state and form fluorescent aggregates in mixed aqueous media.[45,48] On the other hand, ICT phenomena is not observed in case of derivatives **5-7** having electron deficient pyridine groups where aggregation driven-growth and RIR are the reasons of AIEE in these derivatives. Thus, the above results provide another approach to develop materials having high fluorescence efficiency in aggregated state.

Detection of Nitroaromatic Explosives

Recently, detection of nitroaromatic explosives has become an important issue as they are considered to be the environmental contaminants and toxic to the living organisms.[49] Thus, the trace detection of explosives is very important in combating the terrorism, for maintaining the national security and providing the environmental safety.[50-53] The large scale use of explosives by terrorist groups has prompted the scientific community to develop novel sensing materials for their detection. Various methods are available for the detection of nitroaromatics, such as GC-MS, ion-mobility spectroscopy (IMS) surface enhanced Raman spectroscopy and various other spectroscopic techniques.[54-59] However, these methods cannot be used in the field due to their high cost, lack of selectivity and sensitivity.[60] Fluorescence spectroscopy on the other hand is highly sensitive technique hence one of the first choices for the detection of nitroaromatics.[52] In recent years, chemical sensors with high sensitivity for the detection of derivatives such as trinitrotoluene (TNT), dinitrotoluene (DNT), RDX and picric acid (PA), have been reported.[61] However, most of the reported chemosensors work well in organic solvents.[62-66] Thus, the development of sensitive chemosensors for the detection of nitro explosives which work well in aqueous environment is still a challenge.

In view of this, we utilized the fluorescent aggregates of pentacenequinone derivatives **5-9** for the detection of nitroaromatic explosives in mixed aqueous media. For this, we

carried out the fluorescence titrations of derivatives **5-7** in H_2O/DMSO (1:1) and **8/9** in H_2O/THF (9:1) mixtures toward various nitroderivatives such as PA, TNT, DNT, 1,4-dinitrobenzene (DNB), 1,4-dinitrobenzoic acid (DNBA), 1,4-benzoquinone (BQ), nitromethane (NM), and 2,3-dimethyl-2,3-dinitrobutane(DMDNB).

All the pentacenequinone derivatives **5-9** exhibit similar behaviour with nitroaromatic explosives and since pentacenequinone derivative **7** shows higher quantum yield in its aggregate state and thus, we have focused our discussion on the nitroaromatic explosives sensing property of aggregates of derivative **7** in the following discussion. The addition of 58 equiv. of PA to the solution of **7** leads to significant quenching in fluorescence emission (Fig. 4) which is clearly visible to the naked eye under the illumination of UV light of 365 nm (inset, Fig. 4). Similar results were obtained with other pentacenequinone derivatives **5-9** upon addition of PA (Fig. S19-S23 in ESI†) and are summarized in Table 2.

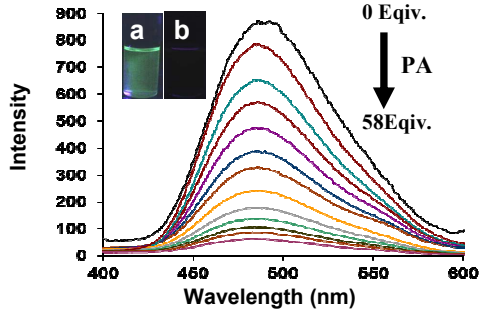

Fig. 4 Change in fluorescence spectra of compound **7** (10 μM) with the addition of PA in H_2O/DMSO (1:1) mixture; inset showing the fluorescence change (a) before and (b) after the addition of PA.

Further, we studied the fluorescence emission response of aggregates of pentacenequinone derivatives **5-9** to PA by using Stern-Volmer relationship. We observed a linear Stern-Volmer plot at lower concentration of PA (Fig. S19-S23 in ESI†) which indicate that fluorescence quenching of aggregates of pentacenequinone derivatives **5-9** involves a static quenching through excited state interaction.[67] However at a higher concentration of PA, the plot bents upwards (Fig. S19-S23 in ESI†), thus, indicating superamplified quenching effect.[68,69] These results suggest that the observed fluorescence quenching of the fluorescent aggregates is attributed to the electron transfer and/or energy transfer quenching mechanism.[53,70] We measured fluorescence life time of aggregates of derivatives **5-9** in the absence and presence of PA (Fig.S24-S28 in ESI†).The fluorescence lifetimes of aggregates of **5-9** were found to be invariant at different concentration of PA thus, indicating that the aggregates of **5-9** decay mainly through the static pathway.[71,72]

Further, the spectral overlap between absorption spectrum of PA and emission spectrum of aggregates in the wavelength region of 420-480 nm (Fig. S29-S33 in ESI†) allows the energy transfer from excited state of aggregates of derivatives **5-9** to ground state to PA, further increases the fluorescence quenching efficiency.[53,73,74] The Stern-Volmer constant of derivative **7** at

Derivative	PA (equiv.)	Stern-Volmer Constant (in M^{-1})	Detection Limit (in nM)
5[a]	62	3.40×10^3	720
6[a]	60	4.36×10^3	650
7[a]	58	6.52×10^3	600
8[b]	40	8.44×10^3	250
9[b]	40	3.61×10^3	290

Table 2. Stern-Volmer constant and detection limit of derivatives 5-9 [a] in H_2O/DMSO (1:1), [b] in H_2O/THF (9:1).

lower concentration of PA is found to be 6.52×10^3 M^{-1}. The detection limit of derivative **7** for PA is calculated to be 600 nM. The better detection level in case of derivative **7** as compared to derivatives **5** and **6** is due to the presence of flake like structure in derivative **7** which is formed by entangled piling of the aggregates (Fig. S9B in ESI†).[75] The flake like structure provides the increase in porosity as well as large surface area which leads to good contact with the explosives and enhances the sensing sensitivity.[75,76] However, in case of derivatives **5** and **6** irregular aggregates are observed (Fig. S4A and S9A in ESI†) which prefer to accumulate in a compact manner which leads to less porosity, hence, lower sensitivity was observed.[75] The Stern-Volmer constants and detection limits for PA with other pentacenequinone derivatives are summarized in Table 2 and lower detection limit in case of derivative **8** indicates that the presence of alkyl chains provides big cavities which allow PA molecules to diffuse more quickly.[47, 77] Thus, derivative **8** shows good sensitivity to PA. The quenching in fluorescence emission of derivatives **5-9** were also observed with TNT, DNT, DNB, DNBA, BQ, NM, and DMDNB. The results of fluorescence studies of derivatives **5-9** with PA, TNT, DNT, DNB, DNBA, BQ, NM, and DMDNB are summarized in Fig. S34 and Fig. S35 in ESI†. From this data we may conclude that fluorescent aggregates of derivatives **5-9** are sensitive for the detection of nitroaromatic explosives.

Further, for practical applications we have utilized the fluorescent aggregates for the detection of nitroaromatic explosives in solid state. For this we prepared test strips by dip-coating solution of pentacenequinone derivatives **5-9** on TLC strips followed by drying the strips under vacuum. TLC strips of AIEE-active pentacenequinone derivatives show strong emission which becomes non-emissive when dipped into aqueous solution of PA which can be observed by naked eye (Fig. 5 and Fig. S36-S39 in ESI†). For detection of very small amounts of PA, we prepared the aqueous solutions of PA of different concentration and 3 μL of each solution were placed on **5-9** test strips (Fig. 6 and Fig. S40-S43 in ESI†).

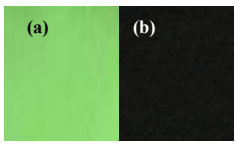

Fig. 5 Photographs of compound **7** on test strips (a) before and (b) after dipping into aqueous solutions of PA.

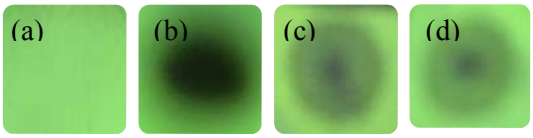

Fig. 6 Photographs (under 365 nm UV light) of fluorescence quenching of aggregates of derivative **7** on test strips for the visual detection of small amount of PA (A) test strip; PA of different concentration (b) 10^{-4} M (c) 10^{-6} M (d) 10^{-8} M.

Dark spots of different strengths were formed, which shows the practically applicability of test strip by varying the concentration of PA even up to 10^{-8} M level. Thus, these results show that derivatives **5-9** are excellent chemosensors for the instant visualization of trace amount of PA in solution as well as in solid state.

Conclusions

In conclusion, we synthesized pentacenequinone derivatives **5-9** by Suzuki-Miyaura coupling strategy. Emission intensity of derivatives **5-7** increased in aggregated state with increase in number of pyridine rotors on pentacenequinone core. Further, fluorescence studies of derivatives **6-7** suggest that aggregation driven-growth along with restriction of intramolecular rotation are the main causes of AIEE phenomenon. On the other hand, derivatives **8-9** having phenyl groups are donor-accepter-donor type systems which exhibit intermolecular charge transfer state and form fluorescent aggregates due to conformational fixation upon aggregate formation in mixed aqueous media. In addition to this, aggregates of derivatives **5-9** can detect nitroaromatic explosives in mixed aqueous media. Pentacenequinone derivative **8** having alkyl chain showed better detection limit as compared to derivative **9,** thus, providing another molecular design for increasing the sensitivity of the molecule. We also utilized TLC strips coated with derivatives **5-9** for instant detection of nitroaromatic explosives which provide simple, portable and low cost method for the detection of nitroaromatic explosives.

Experimental Section

General experimental procedure: please see pS3 in ESI†.

General procedure for the synthesis of derivatives ***5, 7-9****:* (Compound **6** was synthesised by reported method[23])
To a solution of 1/3/2/2 (0.5/0.5/0.5/0.5 g, 1.3/0.80/1.07/2.45 mmol) and 4a/4a/4b/4c (0.293/0.699/0.72/0.457 g, 1.43/3.36/2.25/0.98 mmol) in 20 ml of 1,4-dioxane were added K_2CO_3 (0.359/0.885/1.18/1.08 g, 2.6/6.41/8.56/7.84 mmol), distilled H_2O (1.3/3.2/3/3 mL) and $Pd(Cl)_2(PPh_3)_2$ (0.2/0.123/0.273/0.249 g, 0.286/0.176/0.236/ 0.215 mmol) under N_2, and the reaction mixture was then refluxed overnight. After completion of the reaction (TLC), the mixture was cooled to room temperature. 1,4-dioxane was then removed under vacuum, and the residue so obtained was treated with water, extracted with CH_2Cl_2 and dried over anhydrous Na_2SO_4. The organic layer was evaporated and compound was purified by column chromatography to give compound **5/7/8/9**.

Derivative 5: chloroform/methanol (97:3); 60% yield; M.Pt.>260°C; ^{1}H NMR (300 MHz, $CDCl_3$, ppm): δ = 7.46-7.50 (m, 1H, ArH), 7.70-7.73 (m, 2H, ArH), 7.91-7.95 (m, 1H, ArH), 8.03-8.07 (m, 1H, ArH), 8.11-8.15 (m, 2H, ArH), 8.22-8.30 (m, 2H, ArH), 8.69 (d, 1H, *J* = 3.3 Hz, ArH), 8.95 (s, 2H, ArH), 8.97 (s, 1H, ArH), 9.01 (s, 1H, ArH), 9.02 (s, 1H, ArH); TOF MS ES+: 386.2; Due to poor solubility of compound **5**, its ^{13}C NMR spectrum could not be recorded. Elemental analysis: Calcd. for $C_{27}H_{15}NO_2$: C, 84.14%; H, 3.92%; N, 3.63%; Found: C, 84.05%; H, 3.62%; N, 3.60%.

Derivative 7: chloroform/methanol (97:3); 30% yield; M.Pt.>260°C; ^{1}H NMR (300 MHz, $CDCl_3$, ppm): δ = 7.28 (s, 4H, ArH), 7.49-7.52 (m, 4H, ArH), 8.24 (s, 4H, ArH), 8.59 (s, 8H, ArH), 9.06 (s, 4H, ArH); TOF MS ES+: 617.3 $(M+1)^+$; Due to poor solubility of compound **7**, its ^{13}C NMR spectrum could not be recorded Elemental analysis: Calcd. for $C_{42}H_{24}N_4O_2$: C, 81.80%; H, 3.92%; N, 9.09%; Found: C, 81.75%; H 3.62%; N, 9.00%.

Derivative 8: chloroform/hexane (1:1); 35% yield; M.Pt. >260°C; ^{1}H NMR (300 MHz, $CDCl_3$): δ = 0.92 [t, 6H, *J* = 6.6 Hz, $OCH_2CH_2(CH_2)_3CH_3$], 1.26 [br, 4H, $OCH_2CH_2CH_2CH_2CH_2CH_3$], 1.35-1.37 [m, 4H, $OCH_2CH_2CH_2CH_2CH_2CH_3$], 1.45-1.55 [m, 4H, $OCH_2CH_2CH_2CH_2CH_2CH_3$], 1.79 [t, 4H, *J* = 7.35 Hz, $OCH_2CH_2(CH_2)_3CH_3$], 3.97 [t, 4H, *J* = 6.6 , $OCH_2CH_2(CH_2)_3CH_3$], 6.83 [d, 4H, *J* = 8.7 Hz, ArH], 7.16 [d, 4H, J = 8.7 ArH], 7.69-7.72 [m, 2H, ArH], 8.09 [s, 2H, ArH], 8.11-8.15 (m, 2H, ArH), 8.94 [s, 2H, ArH], 8.95 (s, 2H, ArH); ^{13}C-NMR δ (75.45 MHz, $CDCl_3$): 14.04, 22.62, 25.76, 29.27, 31.62, 68.04, 100.14, 114.49, 129.47, 129.78, 130.08, 130.60, 130.69, 130.95, 131.14, 132.63, 134.40, 135.30, 142.75, 158.53, 182.99; TOF MS ES+: 685.4335 $(M+Na+2)^+$; Elemental analysis: Calcd. for $C_{46}H_{44}O_4$: C 83.60; H 6.71; Found: C 83.55; H 6.60.

Derivative 9: chloroform/Hexane (1:1); 40% yield; M.Pt. >260°C; ^{1}H NMR (300 MHz, $CDCl_3$): δ = 7.29 [s, 2H, ArH], 7.69-7.72 [m, 6H, ArH], 8.11-8.15 [m, 6H, ArH], 8.94 [s, 4H, ArH], 8.97 (s, 2H, ArH). ^{13}C-NMR δ (75.45 MHz, $CDCl_3$): 127.32, 128.13, 129.49, 129.61, 129.81, 129.86, 130.14, 130.41, 130.63, 130.93, 131.46, 135.30, 140.33, 142.97, 183.01. TOF MS ES+: 482.2296 $(M+Na)^+$; Elemental analysis: Calcd. for $C_{32}H_{20}O_2$: C 88.67; H 4.38; Found: C 88.68; H 4.36.

Acknowledgment

VB is highly thankful to DST (Ref. No.SR/S1/OC-63/2010), CSIR (Ref. No. 02(0083)/12/EMR-II) for financial support and Guru Nanak Dev University for providing the research facilities. AG is thankful to CSIR (New Delhi) for senior research fellowship, SK is thankful to DST for INSPIRE fellowship.

Notes and references

Department of Chemistry, UGC Sponsored-Centre for Advanced Studies-I, Guru Nanak Dev University, Amritsar-143005, Punjab, India. Fax: +91 (0)183 2258820; Tel: +91 (0)183 2258802-9 ext. 3202; Email vanmanan@yahoo.co.in
§These authors equally contributed to this work
† Electronic Supplementary Information (ESI) available: [Optical and

spectroscopic data of derivatives **5-9**].
See DOI: 10.1039/b000000x/

1. R. H. Friend, R. W. Gymer, A. B. Holmes, J. H. Burroughes, R. N. Marks, C. Taliani, D. D. C. Bradley, D. A. Dos Santos, J. L. Bredas, M. Logdlund and W. R. Salaneck, *Nature,* 1999, **397**, 121-128.
2. J. Zaumseil and H. Sirringhaus, *Chem. Rev*., 2007, **107**, 1296-1323.
3. A. Kraft, A. C. Grimsdale and A. B. Holmes, *Angew. Chem., Int. Ed.,* 1998, **37**, 402-428.
4. B. K. An, S. K. Kwon, S. D. Jung and S. Y. Park, *J. Am. Chem. Soc*., 2002, **124**, 14410-14415.
5. J. Wang, Y. Zhao, C. Dou, H. Sun, P. Xu, K. Ye, J. Zhang, S. Jiang, F. Li and Y. Wang, *J. Phys. Chem. B,* 2007, **111**, 5082-5089.
6. H. Langhals, O. Krotz, K. Polborn and P. Mayer, *Angew. Chem., Int. Ed*., 2005, **44**, 2427-2428.
7. Z. Xie, B. Yang, F. li, G. Cheng, L. Liu, G. Yang, H. Xu, L. Ye, M. Hanif, S. Liu, D. Ma and Y. Ma, *J. Am. Chem. Soc*., 2005, **127**, 14152-14153.
8. Y. Dong, J. W. Y. Lam, A. Qin, J. Sun, J. Liu, Z. Li, J. Sun, H. H. Y. Sung, I. D. Williams, H. S. Kwok and B. Z. Tang, *Chem. Commun*., 2007, 3255-3257.
9. T. E. Kaiser, H. Wang, V. Stepanenko and F. Wurthner, *Angew. Chem., Int. Ed*., 2007, **119**, 5637-5640.
10. M. Shimizu, Y. Takeda, M. Higashi and T. Hiyama, *Angew. Chem., Int. Ed.,* 2009, **48**, 3653-3656.
11. G. Yu, S. Yin, Y. Liu, J. Chen, X. Xu, X. Sun, D. Ma, X. Zhan, Q. Peng, Z. Shuai, B. Z. Tang, D. Zhu, W. Fang and Y. Luo, *J. Am. Chem. Soc*., 2005, **127**, 6335-6346.
12. J. Chen, H. Peng, C. C. W. Law, Y. Dong, J. W. Y. Lam, I. D. Williams and B. Z. Tang, *Macromolecule,* 2003, **36**, 4319-4327.
13. B. K. An, D. S. Lee, Y. S. Park, H. S. Song and S. Y. Park, *J. Am. Chem. Soc*., 2004, **126**, 10232-10233.
14. F. Wang, M. Y. Han, K. Y. Mya, Y. Wang and Y. H. Lai, *J. Am. Chem. Soc*., 2005, **127**, 10350-10355.
15. K. Itami, Y. Ohashi and J. I. Yoshida, *J. Org. Chem*., 2005, **70**, 2778-2792.
16. H. H. Lin, Y. C. Chan, J. W. Chen and C. C. Chang, *J. Mater. Chem.,* 2011, **21**, 3170-3177.
17. L. Yang, J. Ye, X. Xu, L. Yang, W. Gong, Y. Lin and G. Ning, *RSC Adv*., 2012, **2**, 11529-11535.
18. X. Du and Z. Y. Wang, *Chem. Commun*., 2011, **47**, 4276-4278.
19. X. Zhang, Z. Chi, B. Xu, L. Jiang, X. Zhou, Y. Zhang, S. Liu and J. Xu, *Chem. Commun*., 2012, **48**, 10895-10897.
20. S. J. Yoon, J. W. Chung, J. Gierschner, K. S. Kim, M. G. Choi, D. Kim and S. Y. Park, *J. Am. Chem. Soc*., 2010, **132**, 13675-13683.
21. X. Q. Zhang, Z. G. Chi, B. J. Xu, C. J. Chen, X. Zhou, Y. Zhang, S. W. Liu and J. R. Xu, *J. Mater. Chem*., 2012, **22**, 18505-18513.
22. V. Bhalla, A. Gupta and M. Kumar, *Org. Lett*., 2012, **12**, 3112-3115.
23. V. Bhalla, A. Gupta and M. Kumar, *Chem. Commun*., 2012, **48**, 11862-11864.
24. M. Kumar, V. Vij and V. Bhalla, *Langmuir,* 2012, **28**, 12417-12421.
25. V. Bhalla, S. Pramanik and M. Kumar, *Chem. Commun*., 2013, **49**, 895-897.
26. Y. Hong, J. W. Y. Lam and B. Z. Tang, *Chem. Commun.,* 2009, 4332-4353.
27. I. Salzmann, D. Nabok, M. Oehzelt, S. Duhm, A. Moser, G. Heimel, P. Puschnig, C. A. Draxl, J. P. Rabe and N. Koch, *Cryst. Growth Des*., 2011, **11**, 600-606.
28. Q. Zhao, X. A. Zhang, Q. Wei, J. Wang, X. Y. Shen, A. Qin, J. Z. Sun and B. Z. Tang, *Chem. Commun.,* 2012, **48**, 11671-11673.
29. Q. Zeng, Z. Li, Y. Dong, C. Di, A. Qin, Y. Hong, L. Ji, Z. Zhu, C. K. W. Jim, G. Yu, Q. Li, Z. Li, Y. Liu, J. Qin and B. Z. Tang, *Chem. Commun*., 2007, 70-72.
30. W. Li, D. P. Nelson, M. S. Jensen, R. S. Hoerrner, D. Cai, R. D. Larsen and P. J. Larsen, *J. Org. Chem*., 2002, **67**, 5394-5397.
31. C. R. Swartz, S. R. Parkin, J. E. Bullock, J. E. Anthony, A. C. Mayer and G. G. Malliaras, *Org. Lett.,* 2005, **7**, 3163-3166.
32. K. N. Plunkett, K. Godula, C. Nuckolls, N. Tremblay, A. C. Whalley and S. Xiao, *Org. Lett.,* 2009, **11**, 2225-2228.
33. B. Z. Tang, Y. Geng, J. W. Y. Lam, B. Li, X. Jing, X. Wang, F. Wang, A. B. Pakhomov and X. X. Zhang, *Chem. Mater.,* 1999, **11**, 1581-1589.
34. J. N. Demas and G. A. Grosby, *J. Phys. Chem*., 1971, **75**, 991-1024.
35. S. Jang, S. G. Kim, D. Jung, H. Kwon, J. Song, S. Cho, Y. C. Ko, and H. Sohn, *Bull. Korean Chem. Soc*., 2006, **27**, 12.
36. S. Dong, Z. Li and J. Qin, *J. Phys. Chem. B,* 2009, **113**, 434-441.
37. Y. Kubota, S. Tanaka, K. Funabiki, and M. Matsui, *Org.lett.,* 2012, **14**, 4682-4685.
38. Y. Ren, J. W. Y. Lam, Y. Dong, B. Z. Tang and K. S. Wong, *J. Phys. Chem. B,* 2005, **109**, 1135-1140.
39. H. Tong, Y. Hong, Y. Dong, Y. Ren, M. Haussler, J. W. Y. Lam, K. S. Wong and B. Z. Tang, *J. Phys. Chem. B*, 2007, **111**, 2000- 2007.
40. Y-B. Ruan, A. Depauw and I. Leray, *Org.Biomol.Chem*., 2014, **12**, 4335-4341.
41. C.E. Crespo-Hernandez, B. Cohen, P. M. Hare, and B. Kohler, *Chem. Rev*., 2004, **104**, 1977−2019.
42. H. Lee, C. W. Cone, B. Vanden and A. David, *J. High School Res.*, 2010, 1, 12-19.
43. X. Wang, J. Yan, Y. Zhou and J. Pei, *J. Am. Chem. Soc.,* 2010, **132**, 15872-15874.
44. M. Murata, T. Oyama, S. Watanabe, and Y. Masuda, *J. Org.Chem*., 2000, **65,** 164-168.
45. R. M. Adhikari, B. K. Shah, S. S. Palayangoda and D. C. Neckers, *Langmuir,* 2009**, 25**, 2402-2406.
46. Y. Shigemitsu, T. Mutai, H. Houjou and K. Araki, *J. Phys. Chem. A*, 2012, **116**, 12041−12048.
47. H. Nie, G. Sun, M. Zhang, M. Baumgarten and K. Mullen, *J. Mater. Chem*., 2012, **22**, 2129-2132.
48. S. Choi, J. Bouffardb and Y. Kim, *Chem. Sci*., 2014, **5**, 751–755.
49. M. M. Qasim, B. Moore, L. Taylor, P. Honea, L. Gorb and J. Leszczynski, *Int. J. Mol. Sci*., 2007, **8**, 1234-1264.
50. Z. Z. Rose, C. F. Madigan, T. M. Swager and V. Bulovic, *Nature,* 2005, **434**, 876-879.
51. H. Sohn, M. J. Sailor, D. Magde and W. C. Trogler, *J. Am. Chem. Soc*., 2003, **125**, 3821-3830.
52. D. T. McQuade, A. E. Pullen and T. M. Swager, *Chem. Rev*., 2000, **100**, 2537-2574.
53. S. W. Thomas III., G. D. Joly and T. M. Swager, *Chem. Rev*., 2007, **107**, 1339-1386.
54. D. S. Moore, *Rev. Sci. Instrum*., 2004, **75**, 2499-2513.
55. A. W. Czarnik, *Nature,* 1998, **394**, 417-418.
56. K. R. Hakansson, V. Coorey, R. A. Zubarev, V. L. Talrose and P. Hakansson, *J. Mass Spectrom*., 2000, **35**, 337-346.
57. J. M. Sylvia, J. A. Janni, J. D. Klein and K. M. Spencer, *Anal. Chem*., 2000, **72**, 5834-5840.
58. V. P. Anferov, G. V. Mozjoukhine and R. Fisher, *Rev. Sci. Instrum*., 2000, **71**, 1656.
59. R. D. Luggar, M. J. Farquharson, J. A. Horrocks and R. J. Lacey, *X-Ray Spectrom*., 1998, **27**, 87-94.
60. E. Wallis, T. M. Griffin, N. Popkie, M. A. Eagan, R. F. Mcatee, D. Vrazel and J. McKinly, *Proc. SPIE,* 2005, **54**, 5795.
61. M. E. Germain and M. Knapp, *J. Chem. Soc. Rev.,* 2009, **38**, 2543-2555.
62. A. Rana and P. K. Panda, *RSC Adv.,* 2012, **2**, 12164-12168.
63. N. Venkatramaiah, S. Kumar and S. Patil, *Chem. Eur. J.,* 2012, **18**, 14745-14751.
64. S. Shanmugaraju, D. Samanta, B. Gole and P. S. Mukherjee, *Dalton Trans*., 2011, **40**, 12333-12341.
65. Y. H. Lee, H. Liu, J. Y. Lee, S. H. Kim, S. K. Kim, J. L. Sessler, Y. Kim and J. S. Kim, *Chem. Eur. J.,* 2010, **16**, 5895-5901.
66. N. Venkatramaiah, S. Kumar and S. Patil, *Chem. Commun.,* 2012, **48**, 5007-5009.
67. D. Zhao and T. M. Swager, *Macromolecules,* 2005, **38**, 9377-9384.
68. J. Wang, J. Mei, W. Yuan, P. Lu, A. Qin, J. Sun, Y. Ma and B. Z. Tang, *J. Mater. Chem*. 2011, **21**, 4056-4059.
69. D. Li, J. Liu, R. T. K. Kwok, Z. Liang, B. Z. Tang and J. Yu, *Chem. Commun*., 2012, **48**, 7167-7169.
70. Z. F. An, C. Zheng, R. F. Chen, J. Yin, J. J. Xiao, H. F. Shi, Y. Tao, Y. Qian, and W. Huang, *Chem. Eur. J*., 2012, **18**, 15655 – 15661.

71 H. Sohn, M. J. Sailor, D. Magde, and W. C. Trogler, *J. Am. Chem. Soc.,* 2003, **125**, 3821-3830.
72 Y. Long, H. Chen, Y. Yang, H. Wang, Y. Yang, N. Li, K. Li, J. Pei, and F. Liu., *Macromolecules.,* 2009, **42**, 6501–6509
73 W. Wu, S. Ye, L. Huang, L. Xiao, Y. Fu, Q. Huang, G. Yu, Y. Liu, J. Qin, Q. Lia and Z. Li, *J. Mater. Chem*., 2012, **22**, 6374-6382.
74 A. Qin, J. W. Y. Lam, L. Tang, C. K. W. Jim, H. Zhao, J. Sun and B. Z. Tang, *Macromolecules,* 2009, **42**, 1421-1424.
75 X. Liu, X. Zhang, R. Lu, P. Xue, D. Xu and H. Zhou, *J. Mater. Chem.,* 2011, **21**, 8756-8765.
76 Z. Ding, Q. Zhao, R. Xing, X. Wang, J. Ding, L. Wang and Y. Han, *J. Mater. Chem. C,* 2013, **1**, 786-792.
77 H. Li, J. X. Wang, Z. L. Pan, L. Y. Cui, L. Xu, R. M. Wang, Y. L. Song and L. Jiang, *J. Mater. Chem*., 2011, **21**, 1730-1735.

TOC

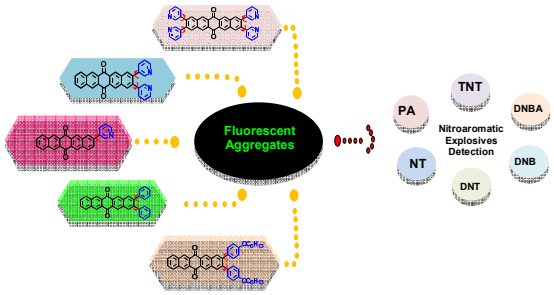

Fluorescent aggregates of AIEE active pentacenequinone based derivatives have been prepared and utilized for selective detection of picric acid.